Contribution from the Department of Chemistry,
University of California, Davis, California 95616

Formation of Luminescent, Metal–Metal Bonded, 3:5 Complexes Using Palladium(II) or Platinum(II) and Iridium(I) through Chelate Ring Openings

Alan L. Balch* and Vincent J. Catalano†

Received March 26, 1992

Treatment of $Pd(NCC_6H_5)_2Cl_2$ or K_2PtCl_4 with 2 equiv of dpmp (dpmp is bis((diphenylphosphino)methyl)phenylphosphine) and ammonium hexafluorophosphate yields yellow $[Pd(dpmp)_2](PF_6)_2$ or colorless $[Pt(dpmp)_2](PF_6)_2$, respectively. $[Pd(dpmp)_2](PF_6)_2$ crystallizes in two forms; yellow crystals of $[Pd(dpmp)_2](PF_6)_2 \cdot 0.5CH_2Cl_2$ form in the monoclinic space group $P2_1/n$ (No. 14) with a = 12.494 (3) Å, b = 36.639 (15) Å, c = 13.912 (5) Å, and β = 90.05 (3)° at 130 K with Z = 4. Refinement of 5487 reflections and 448 parameters gave R = 0.085 and R_w = 0.10. Apricot colored crystals of $[Pd(dpmp)_2](PF_6)_2 \cdot (CH_3CH_2)_2O$ form in the monoclinic space group $C2/c$ (No. 15) with a = 48.88 (2) Å, b = 13.731 (4) Å, c = 21.387 (7) Å, and β = 95.79 (3)° at 130 K with Z = 8. Refinement of 7502 reflections and 466 parameters gave R = 0.085 and R_w = 0.114. Both structures consist of the nearly identical cation, $[Pd(dpmp)_2]^{2+}$. The cation contains a square-planar palladium ion with the two dpmp ligands forming both a four-membered and a six-membered chelate ring. Treatment of $[Pd(dpmp)_2](PF_6)_2$ with either $Ir(CO)Cl(AsPh_3)_2$ or $Ir(CO)Cl(PPh_3)_2$ yields the 3:5 complex $[PdIr(CO)Cl(\mu\text{-dpmp})_2](PF_6)_2$. Red/orange crystals of $[PdIr(CO)Cl(\mu\text{-dpmp})_2](PF_6)_2 \cdot CHCl_3 \cdot CH_3OH$ form in the chiral space group $P2_1$ (No. 4) with a = 13.043 (3) Å, b = 19.214 (4) Å, c = 14.052 (3) Å, and β = 90.78 (3)° at 130 K with Z = 2. Refinement of 2821 reflections and 424 parameters gave R = 0.050 and R_w = 0.061. The cation consists of an 18e⁻ Ir center bonded to a 16e⁻ Pd center at a distance of 2.694 (2) Å. A dichloromethane solution of $[PdIr(CO)Cl(\mu\text{-dpmp})_2](PF_6)_2$ shows a strong absorbance at 458 nm (ϵ = 11 000 M^{-1} cm^{-1}) which is assigned to the $\sigma_{M-M} \rightarrow \sigma^*_{M-M}$ transition. Excitation into this band results in a moderate emission at 520 nm (fluorescence) at 25 °C. Freezing to −196 °C produces emission at 665 nm (phosphorescence). The phosphorescent lifetime was measured at 5 μs while the fluorescent lifetime was <350 ns. Similarly addition of $Ir(CO)Cl(AsPh_3)_2$ or $Ir(CO)Cl(PPh_3)_2$ to $[Pt(dpmp)_2](PF_6)_2$ leads to the formation of yellow $[PtIr(CO)Cl(\mu\text{-dpmp})_2](PF_6)_2$. Yellow crystals of $[PtIr(CO)Cl(\mu\text{-dpmp})_2](PF_6)_2 \cdot 0.75CH_2Cl_2$ form in the monoclinic space group $P2_1/c$ (No. 14) with a = 18.620 (14) Å, b = 18.195 (13) Å, c = 20.539 (7) Å, and β = 94.03 (5)° at 130 K with Z = 4. Refinement of 9071 reflections and 506 parameters yielded R = 0.069 and R_w = 0.080. The Ir–Pt single bond distance is 2.730 (2) Å. The structure of $[PtIr(CO)Cl(\mu\text{-dpmp})_2](PF_6)_2$ differs from that of $[PdIr(CO)Cl(\mu\text{-dpmp})_2](PF_6)_2$ in the relative orientation of the dpmp ligands. The absorption spectrum of $[PtIr(CO)Cl(\mu\text{-dpmp})_2](PF_6)_2$ shows a band at 382 nm (ϵ = 19 000 M^{-1} cm^{-1}). At 25 °C there is a moderate emission at 443 nm (fluorescence), and upon freezing to −196 °C, the 443-nm emission disappears, and a new emission at 670 nm (phosphorescence) appears. The phosphorescent lifetime is 27 μs while the 443-nm emission is <350 ns.

Introduction

Constructing new transition-metal assemblages from mononuclear components using polyfunctional phosphine ligands as backbones allows creation of new environments well suited for exploring the nature of metal–metal bonding.[1,2] The process also calls for developing new reactions suitable for forming these assemblages. In this article we continue our exploration of the chelate ring opening reactions that involve the triphosphine ligand bis((diphenylphosphino)methyl)phenylphosphine, dpmp.[3,4] Complexes containing a single, six-membered chelating dpmp ligand react with other metal ions as a simple phosphine (eq 1) to form complexes in which the chelate ring remains intact, and the various metal centers are well separated.[5] However, complexes

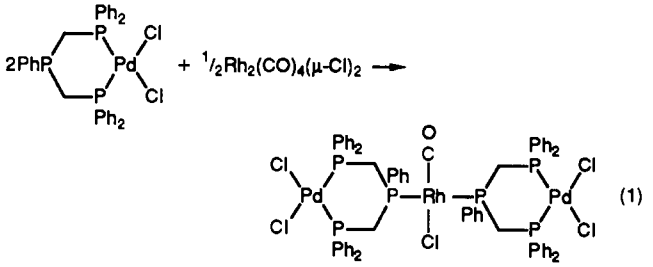

(1)

containing two dpmp ligands can adopt a structure with one six-membered and one four-membered ring.[6,7] These undergo reactions with other metal complexes in which considerable reorganization occurs and, frequently, metal–metal bonds form. An example is shown in eq 2.[7] Here we report the first preparations of $[Pd(dpmp)_2]^{2+}$ and $[Pt(dpmp)_2]^{2+}$, their structural characterization, and their use in constructing binuclear complexes with another d^8 metal ion, iridium(I), through chelate ring openings. The nature of the products of these reactions touches upon another theme of our work, the nature of metal–metal bonding in complexes of two d^8 metal ions.

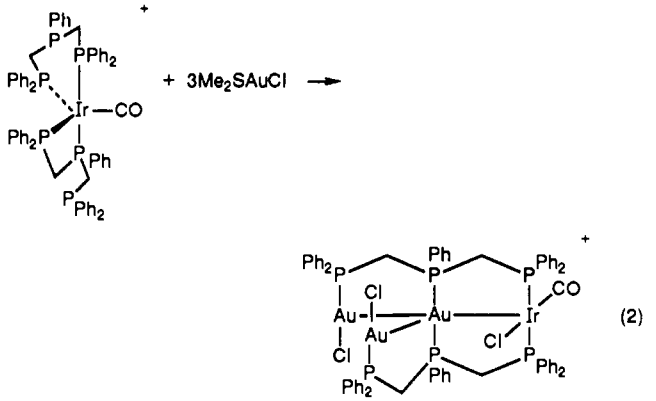

(2)

Complexes containing two d^8 metal centers bound closely together frequently adopt the 4:4 or face-to-face structure A. The 3:5 structure B is a closely related alternative.[8] Compounds of

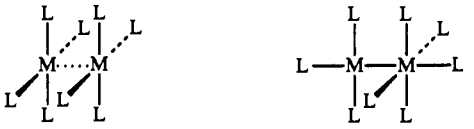

A, 4:4 B, 3:5

the 4:4 type such as $Pt_2(POP)_4^{4-}$ (POP is $P_2O_5H_2^{2-}$) have received considerable attention because of their novel long-lived excited-

† Present address: Department of Chemistry, California Institute of Technology, Pasadena, CA 91125.

(1) Balch, A. L. In *Homogeneous Catalysis with Metal Phosphine Complexes*; Pignolet, L. H., Ed.; Plenum Press: New York, 1983, p 67.
(2) Balch, A. L. *Pure Appl. Chem.* **1988**, *60*, 555.
(3) Guimerans, R. R.; Olmstead, M. M.; Balch, A. L. *J. Am. Chem. Soc.* **1983**, *105*, 1677.
(4) Appel, R.; Geisler, K.; Schöler, H.-F. *Chem. Ber.* **1979**, *112*, 648.
(5) Balch, A. L.; Guimerans, R. R.; Linehan, J. *Inorg. Chem.* **1985**, *24*, 290.
(6) Balch, A. L.; Catalano, V. J.; Olmstead, M. M. *J. Am. Chem. Soc.* **1990**, *112*, 2010.
(7) Balch, A. L.; Catalano, V. J.; Noll, B. C.; Olmstead, M. M. *J. Am. Chem. Soc.* **1990**, *112*, 7558.
(8) Balch, A. L.; Catalano, V. J. Submitted for publication.

0020-1669/92/1331-2569$03.00/0

Scheme I

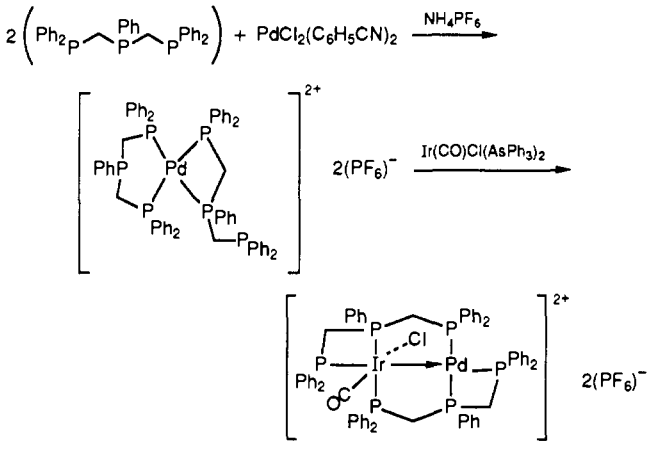

state properties.[9,10] Complexes of the 3:5 type have received much less attention, since they are much less common. In addition to the variations in distribution of ligands, these two structural types show other differences. The metal–metal separations in the 3:5 type are typical of metal–metal single bonds (ca. 2.7 Å for Pd–Rh)[8], but they are longer in the 4:4 type (typically 2.9–3.2 Å). The electronic spectra of the 4:4 complexes are dominated by intense, proximity shifted transitions generally in the visible region that result from excitation from the filled $\sigma^*(d_{z^2}d_{z^2})$ to an empty $\sigma(p_zp_z)$ orbital. These complexes are frequently strongly emissive.[9-12] In contrast, the 3:5 compounds lack the proximity shifted band. In a representative example, $[(CH_3NC)PtRh(CNCH_3)_3(\mu\text{-dpm})_2]^{3+}$ (dpm is bis(diphenylphosphino)methane), the lowest electronic absorption, which may be the $\sigma \rightarrow \sigma^*$ transition, occurs at ca. 290 nm.[8] For these 3:5 complexes, alteration of the two ligands trans to the metal–metal bond produces marked changes in the absorption spectra. Here we describe two new examples of complexes with the 3:5 structure. These are the first of this structural type to show luminescence.

Results

Synthetic Studies. The synthetic results are summarized in Scheme I. Treatment of $Pd(NCPh)_2Cl_2$ with 2 equiv of dpmp in hot ethanol followed by the addition of a methanol solution of ammonium hexafluorophosphate and recrystallization from dichloromethane/ethyl ether produces yellow crystals of $[Pd(dpmp)_2](PF_6)_2 \cdot 0.5CH_2Cl_2$, **1**. Addition of ethyl ether to the mother liquor gave apricot crystals of a second crystalline modification, $[Pd(dpmp)_2](PF_6)_2 \cdot (CH_3CH_2)_2O$, **1′**. Dissolution of the apricot-colored **1′** in dichloromethane produced a yellow solution from which yellow crystals of **1** could be obtained by precipitation with ethyl ether. Addition of 2 equiv of dpmp to a solution of $K_2[PtCl_4]$ in ethanol followed by the addition of a solution ammonium hexafluorophosphate in methanol produces colorless crystals of $[Pt(dpmp)_2](PF_6)_2$, **2**.

The reaction of equimolar amounts to $[Pd(dpmp)_2](PF_6)_2$ and $Ir(CO)Cl(AsPh_3)_2$ in acetone produces a red-orange solution from which red-orange crystals of $[PdIr(CO)Cl(\mu\text{-dpmp})_2](PF_6)_2$, **3**, were obtained by the addition of a solution of ammonium hexafluorophosphate in methanol. Complex **3** can also be obtained from a mixture of **1** and $Ir(CO)Cl(PPh_3)_2$, but the solution must be heated under reflux to obtain a satisfactory conversion to the product. Similarly, treatment of $[Pt(dpmp)_2](PF_6)_2$ with $Ir(CO)Cl(AsPh_3)_2$ in boiling acetone followed by precipitation with ammonium hexafluorophosphate produces yellow crystals of $[PtIr(CO)Cl(\mu\text{-dpmp})_2](PF_6)_2$, **4**. Both **3** and **4** are soluble in acetone, dichloromethane, and chloroform, slightly soluble in methanol, and insoluble in ethyl ether and hydrocarbons.

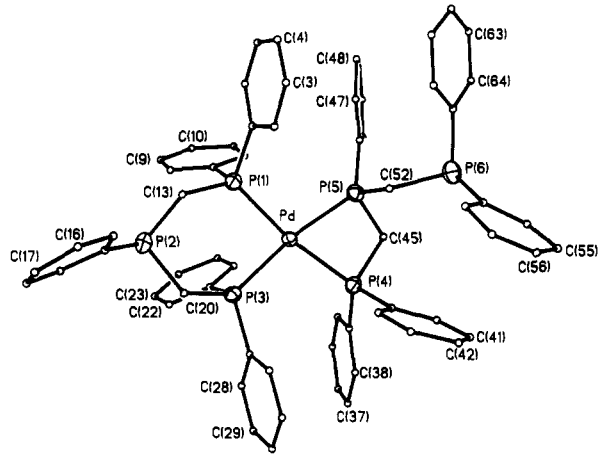

Figure 1. Structure of the cation in $[Pd(dpmp)_2](PF_6)_2$ (**1**) with 50% thermal contours for the heavy atoms and uniform, arbitrarily sized circles for the carbon atoms of the dpmp ligands.

Table I. Selected Interatomic Distances in $[Pd(dpmp)_2](PF_6)_2$ (**1** and **1′**)

	1	**1′**
	Distances, Å	
Pd–P(1)	2.339 (4)	2.332 (2)
Pd–P(3)	2.328 (4)	2.332 (2)
Pd–P(4)	2.359 (4)	2.346 (2)
Pd–P(5)	2.349 (4)	2.374 (2)
	Angles, deg	
P(1)–Pd–P(3)	90.2 (1)	93.2 (1)
P(1)–Pd–P(4)	168.8 (1)	168.3 (1)
P(3)–Pd–P(4)	98.7 (1)	96.6 (1)
P(1)–Pd–P(5)	99.9 (1)	98.6 (1)
P(3)–Pd–P(5)	167.9 (1)	167.2 (1)
P(4)–Pd–P(5)	70.6 (1)	71.1 (1)

Structures of $[Pd(dpmp)_2](PF_6)_2 \cdot 0.5CH_2Cl_2$ (1) and $[Pd(dpmp)_2](PF_6)_2 \cdot (CH_3CH_2)_2O$ (1′). The asymmetric unit of **1** consists of the cation, one ordered and one disordered hexafluorophosphate, and a dichloromethane molecule which is present at 50% occupancy. There are no unusual interactions between these moieties. The structure of the cation is shown in Figure 1. Selected interatomic distances and angles are given in Table I.

The cation contains a palladium ion coordinated by four phosphorus atoms in a nearly planar array. However, the two dpmp ligands are bound differently. One forms a six-membered chelate ring with a pseudo chair geometry and the central phosphorus atom uncoordinated. The shape of this chelate ring resembles that in $Pd(dpmp)Cl_2$.[13] The other dpmp forms a four-membered chelate ring with one of the terminal phosphorus atoms uncoordinated. The P–Pd–P angles within the chelate rings are, as expected, quite different. The P(1)–Pd–P(3) angle in the six-membered ring is 90.2 (3)°, while the P(2)–Pd–P(4) angle in the four-membered ring is 70.6 (1)°. However, the sum of the four P–Pd–P angles (359.4°) is nearly 360°, and so the palladium atom has planar coordination.

The apricot-colored crystals of $[Pd(dpmp)_2](PF_6)_2 \cdot (CH_3CH_2)_2O$, **1′**, contain one cation, two hexafluorophosphate ions, and a molecule of ethyl ether within their asymmetric unit. The structure of the cation is nearly identical to that described above for **1**. Selected interatomic distances and angles for **1′** are given in Table I where they can be compared to those of **1**. Further details regarding this structure are given in the supplementary material.

Structures of $[PdIr(CO)Cl(\mu\text{-dpmp})_2](PF_6)_2 \cdot CHCl_3 \cdot CH_3OH$ (3) and $[PtIr(CO)Cl(\mu\text{-dpmp})_2](PF_6)_2 \cdot 0.75CH_2Cl_2$ (4). The asym-

(9) Roundhill, D. M.; Gray, H. B.; Che, C.-M. *Acc. Chem. Res.* **1989**, *22*, 55.
(10) Zipp, A. P. *Coord. Chem. Rev.* **1988**, *84*, 47.
(11) Fordyce, W. A.; Crosby, G. A. *J. Am. Chem. Soc.* **1982**, *104*, 985.
(12) Marshall, J. L.; Stobart, S. R.; Gray, H. B. *J. Am. Chem. Soc.* **1984**, *106*, 3027.
(13) Olmstead, M. M.; Guimerans, R. R.; Farr, J. P.; Balch, A. L. *Inorg. Chim. Acta* **1983**, *75*, 199.

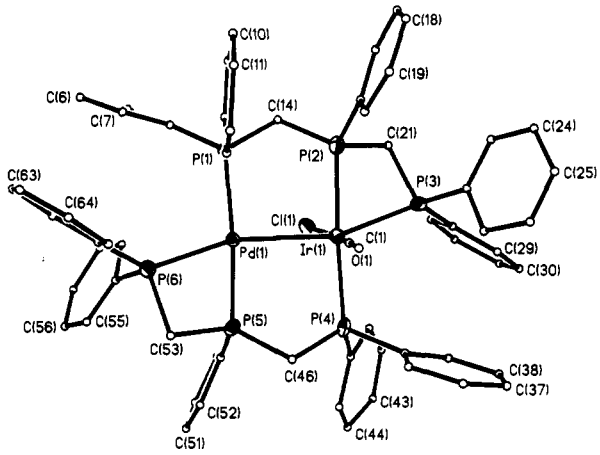

Figure 2. Structure of the cation in $[PdIr(CO)Cl(\mu\text{-dpmp})_2](PF_6)_2$ (**3**).

Table II. Selected Interatomic Distances and Angles in $[PdIr(CO)Cl(\mu\text{-dpmp})_2](PF_6)_2$ (**3**) and $[PtIr(CO)Cl(\mu\text{-dpmp})_2](PF_6)_2$ (**4**)

	3 (M = Pd)	4 (M = Pt)
	Distances, Å	
M–Ir	2.694 (2)	2.730 (2)
M–P(1)	2.333 (7)	2.340 (5)
M–P(5)	2.264 (6)	2.256 (5)
M–P(6)	2.306 (6)	2.303 (5)
Ir–P(2)	2.361 (7)	2.338 (5)
Ir–P(3)	2.414 (7)	2.410 (6)
Ir–P(4)	2.370 (6)	2.370 (6)
Ir–C(1)	1.82 (3)	1.84 (2)
Ir–Cl(1)	2.405 (8)	2.417 (5)
P(1)···P(2)	2.885 (11)	2.970 (10)
P(2)···P(3)	2.713 (11)	2.743 (10)
P(4)···P(5)	2.882 (11)	2.994 (10)
P(5)···P(6)	2.648 (11)	2.710 (10)
	Angles, deg	
M–Ir–P(2)	91.9 (2)	91.0 (1)
M–Ir–P(3)	156.4 (2)	158.1 (1)
M–Ir–P(4)	92.7 (2)	94.2 (2)
P(2)–Ir–C(1)	95.6 (8)	99.6 (7)
P(2)–Ir–Cl(1)	83.9 (2)	85.3 (2)
P(3)–Ir–C(1)	94.1 (8)	87.6 (7)
P(3)–Ir–Cl(1)	88.2 (2)	89.4 (2)
P(4)–Ir–C(1)	86.0 (8)	91.0 (7)
P(4)–Ir–Cl(1)	95.4 (3)	85.8 (2)
C(1)–Ir–Cl(1)	169.4 (8)	163.9 (7)
P(2)–Ir–P(3)	69.2 (2)	70.5 (2)
P(2)–Ir–P(4)	175.1 (2)	168.4 (2)
P(3)–Ir–P(4)	105.9 (2)	101.9 (2)
P(5)–M–P(6)	70.8 (2)	72.9 (2)
M–Ir–C(1)	94.1 (8)	87.6 (7)
M–Ir–Cl(1)	75.4 (2)	76.9 (1)
Ir(1)–M–P(1)	92.7 (2)	93.8 (1)
Ir(1)–M–P(5)	91.9 (2)	89.9 (1)
Ir(1)–M–P(6)	161.4 (2)	158.2 (1)
P(1)–M–P(5)	175.1 (2)	174.3 (2)
P(1)–M–P(6)	104.4 (2)	102.4 (2)

metric unit of $[PdIr(CO)Cl(\mu\text{-dpmp})_2](PF_6)_2 \cdot CHCl_3 \cdot CH_3OH$ contains the cation, two entirely normal hexafluorophosphate anions, one molecule of chloroform, and one molecule of methanol. There are no unusual contacts between these subunits. Figure 2 shows a drawing of the cation. Table II contains selected interatomic distances and angles.

The cation consists of a five-coordinate iridium ion bonded to a three-coordinate palladium ion. The Ir–Pd distance, 2.694 (2) Å, is consistent with the presence of a single bond between these. As found for many phosphine-bridged complexes with the metal–metal bonds,[14] this distance is shorter than the nonbonded P···P separations (P(1)···P(2), 2.885 (11) Å; P(4)···P(5), 2.990 (11) Å) that are involved in the ligand bridges that surround the two metal ions.

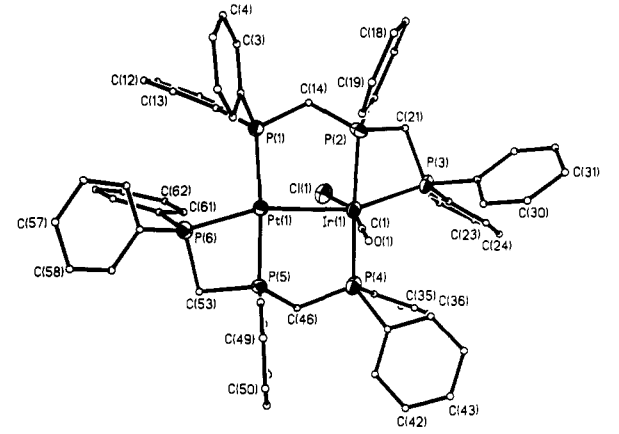

Figure 3. Structure of the cation in $[PtIr(CO)Cl(\mu\text{-dpmp})_2](PF_6)_2$ (**4**). Notice that from this vantage point the orientation of the upper dpmp is nearly identical to that shown in Figure 2. However, careful inspection reveals that the phenyl group on P(5) projects toward the viewer in this figure while it projects away in Figure 2.

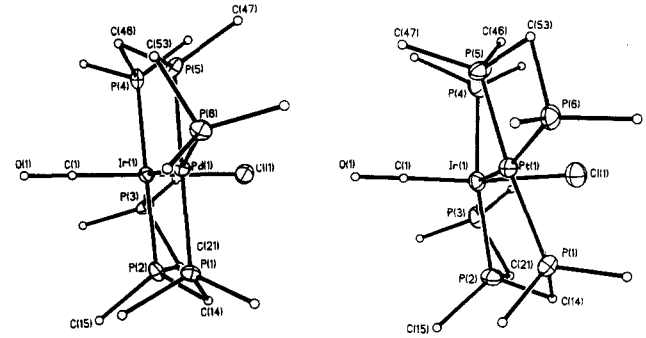

Figure 4. Comparison of the inner cores of $[PdIr(CO)Cl(\mu\text{-dpmp})_2](PF_6)_2$ (**3**) (left) and $[PtIr(CO)Cl(\mu\text{-dpmp})_2](PF_6)_2$ (**4**) (right).

The two dpmp are inequivalent but function similarly. Each uses a terminal and an internal phosphorus atom to bridge the Pd–Ir bond. One also forms a four-membered chelate ring about the iridium ion while the other forms a four-membered chelate ring about palladium. The presence of these chelate rings distorts the structure from the ideal 3:5 structure. While the P(1)PdP(5)IrP(2)P(4)Cl(1)C(1) unit has regular, rectilinear geometry, the locations of the remaining phosphorus atoms, P(3) and P(6), are positioned so that the P(6)PdIrP(3) group is nonlinear. The Pd–Ir–P(3) angle is 156.4 (2)° and the Ir–Pd–P(6) angle is 161.4 (2)°. While the angles involving the phosphine ligands in cis orientations on Pd and Ir are in the ranges 91.9–92.7°, the P(2)–Ir–P(3) and P(5)–Pd–P(6) angles, which involve the chelate rings, are 69.2 (2)° and 70.8 (2)°, respectively. The metal–ligand bond lengths all fall within normal ranges.

The asymmetric unit of $[PtIr(CO)Cl(\mu\text{-dpmp})_2](PF_6)_2 \cdot 0.75CH_2Cl_2$, **4**, contains the cation, two entirely normal hexafluorophosphate anions, and three-fourths of a badly disordered dichloromethane molecule. Selected interatomic distances and angles are given in Table II where they may be compared to those of **3**.

A drawing showing the structure of the cation in **4** is shown in Figure 3. The cation belongs to the 3:5 structural type. It has considerable similarity to the cation in **3**. The Ir–Pt distance, 2.730 (2) Å, is comparable to but slightly longer than the Ir–Pd distance in **3**. The two dpmp ligands function as bridging and chelating ligands, and each is unique. However, their relative orientations are different from those found in **3**. These differences results from changes in the configuration at P(5). This is best seen by turning to Figure 4 which shows the cores of the cations of **3** and **4** with all but the ipso carbon atoms of the phenyl rings removed. In **3** the C(46)P(4)P(5)P(2)P(1)C(14) ring has a

(14) Olmstead, M. M.; Lindsay, C. H.; Benner, L. S.; Balch, A. L. *J. Organomet. Chem.* **1979**, *179*, 289.

Table III. Crystal Data and Data Collection Parameters

	1	1′	3	4
formula	$C_{64.25}H_{58}Cl_{0.5}F_{12}P_8Pd$	$C_{68}H_{58}F_{12}P_8PdO$	$C_{67}H_9Cl_4F_{12}P_8Pd$	$C_{65.25}H_{58}Cl_{2.25}F_{12}IrOP_8Pt$
fw	1430.0	1473.3	1761.9	1800.95
color and habit	yellow blocks	apricot blocks	red/gold parallelepipeds	yellow pyramids
crystal system	monoclinic	monoclinic	monoclinic	monoclinic
space group	$P2_1/n$ (No. 14)	$C2/c$ (No. 15)	$P2_1$ (No. 4)	$P2_1/c$ (No. 14)
a, Å	12.494 (3)	48.88 (2)	13.043 (3)	18.620 (14)
b, Å	36.639 (15)	13.731 (4)	19.214 (4)	18.195 (13)
c, Å	13.912 (5)	21.387 (7)	14.052 (3)	20.539 (7)
β, deg	90.05 (3)	95.79 (3)	90.78 (3)	94.03 (5)
V, Å^3	6388 (4)	14281 (8)	3521.1 (13)	6941 (8)
T, K	130	130	130	130
Z	4	8	2	4
d_{calcd}, g cm^{-3}	1.487	1.370	1.662	1.720
radiation, Å	0.71073	0.71073	0.71073	0.71073
μ(Mo Kα), mm^{-1}	0.92	0.501	2.54	2.15
range of transm factors	0.51–0.85	0.51–0.71	0.23–0.84	0.31–0.43
R^a	0.085	0.087	0.051	0.070
$R_w{}^a$	0.103	0.114	0.060	0.079

$^a R = \sum||F_o| - |F_c||/|F_o|$ and $R_w = \sum||F_o| - |F_c||w^{1/2}/\sum|F_o|w^{1/2}$.

chairlike geometry which places the methylene carbons on opposite sides of the Ir–Pd bond. In **4** this ring has a boatlike geometry that positions methylene groups on the same side of the Ir–Pt bond. These differences result in different degrees of twisting of the P(1)–M–P(5) units relative to the P(2)–Ir–P(4) unit. In **3** there is little twist with the torsional angles defined by P(1)–Pd–Ir–P(2) and P(5)–Pd–Ir–P(4) assuming small values (3.0 (3)° and 0.4 (3)°, respectively). In **4** the twist is greater, and the torsional angles (P(1)–Pt–Ir–P(2) and P(5)–Pt–Ir–P(4)) expand to 12.2 (2)° and 18.3 (2)°, respectively. The arrangement present in **3** places five phenyl rings and the carbon monoxide ligand on one side of the face defined by IrPdP(1)P(2)P(4)P(5) and five phenyl rings and the chloride ligand on the opposite face. In **4** however, there are six phenyl rings and a carbon monoxide ligand protruding from one face to the surface defined by IrPtP(1)P(2)P(4)P(5) while four phenyl rings and the chloride ligand project from the opposite side of that surface. The two distinct orientations of the two dpmp ligands seen in **3** and **4** cannot be interchanged by simple bond rotations. Breaking of metal–P bonds is required to convert one arrangement into another.

Despite these variations in the overall structures of **3** and **4**, individual bond distances and angles in these two complex cations are remarkably similar as inspection of Table III will show.

$^{31}P\{^1H\}$ NMR Spectra. The $^{31}P\{^1H\}$ NMR spectra of these complexes indicate that each retains the gross structure which is present in the solid state. The spectrum for **1** recorded in $CDCl_3$ at 23 °C is shown in Figure 5. Four groups of resonances, A–D, are observed. On the basis of their chemical shift and relative intensity, the group A is assigned to P(1) and P(3) which are part of the six-membered chelate rings. Such rings typically show ^{31}P chemical shifts of 0 to 20 ppm.[5] Four-membered chelate rings for d^8 metals usually produce upfield shifts[15] so that the group of resonances B are assigned to P(5) and P(4). The chemical shift differences between P(1) and P(3) and between P(5) and P(4) are small; thus the spectrum has a deceptively simple appearance. Resonance C is assigned to the uncoordinated phosphorus P(6) while D is assigned to P(2). The $^{31}P\{^1H\}$ COSY spectrum of this sample reveals that resonance D is coupled only to A while C is coupled only to B, thus verifying these assignments. The experimental spectrum also shows a number of peaks of lower intensity which are present in all samples of this complex. They probably arise from another isomer of the complex or an oligomeric form. Oligomer formation has been observed previously with metal complexes that contain uncoordinated phosphorus donors.[5,6]

The $^{31}P\{^1H\}$ NMR spectrum of $[PtIr(CO)Cl(\mu\text{-dpmp})_2](PF_6)_2$ is shown in Figure 6. Six major resonances (labeled A through F) of equal intensity are observed along with a set of minor

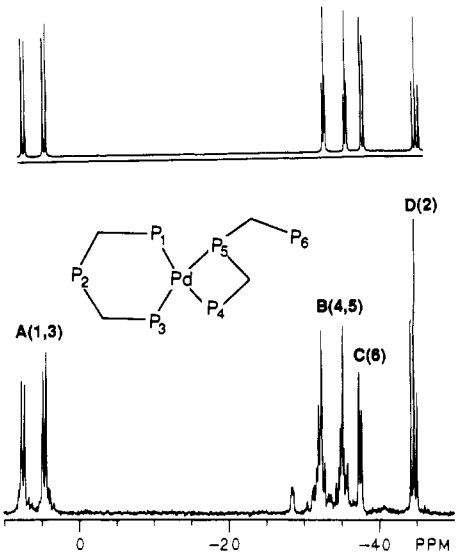

Figure 5. The 121.7-MHz $^{31}P\{^1H\}$ NMR spectrum of $[Pd(dpmp)_2](PF_6)_2$ in acetone-d_6 at 25 °C, and simulated spectrum using δ_1 = 6.4 ppm, δ_3 = 6.5 ppm, δ_4 = −33.8 ppm, δ_5 = −33.8 ppm, δ_6 = −37.5 ppm, and δ_2 = −44.7 ppm with $J(1,2)$ = 50 Hz, $J(1,4)$ = 350 Hz, $J(3,5)$ = 350 Hz, $J(2,3)$ = 50 Hz, and $J(5,6)$ = 46 Hz.

resonances. The major resonances can be assigned to structure with the basic skeletal unit which was determined crystallographically. Resonances B and E form a basic AB quartet with $^2J_{(P,P)}$ = 359 Hz with further fine structure. Both resonances lack satellites due to coupling to ^{195}Pt (spin $^1/_2$; 33.4% natural abundance). Therefore, they can be assigned to P(2) and P(4) whose cis relationship to the Ir–Pt bond makes the two-bond Pt–P coupling very small. Resonance F shows ^{195}Pt satellites with a coupling constant of 485 Hz. This is too small to represent a one-bond coupling but is entirely consistent with a two bond coupling if the Pt–Ir–P unit has a trans relationship. Consequently resonance F is assigned to P(3). The remaining resonances have satellites that are indicative of one-bond Pt–P coupling. Resonances A and C can be assigned to the trans phosphorus atoms, P(1) and P(5). The large P–P coupling constant, 400 Hz, is consistent with the trans arrangement of these two atoms. This leaves resonance D to be assigned to P(6). A satisfactory simulation of the spectrum with minor P–P couplings consistent with the structure along with the parameters used are given in Figure 6 and its caption. The minor resonances shown in Figure 6 are present in all samples of **4** that we have made. Their intensities do not decrease during purification. The observable resonances seem to follow a pattern that is similar to those of the major resonances, but there is sufficient overlapping of these resonances,

(15) Hunt, C. T.; Balch, A. L. *Inorg. Chem.* **1982**, *21*, 1641.
(16) Guimerans, R. R.; Olmstead, M. M.; Balch, A. L. *Inorg. Chem.* **1983**, *22*, 2223.

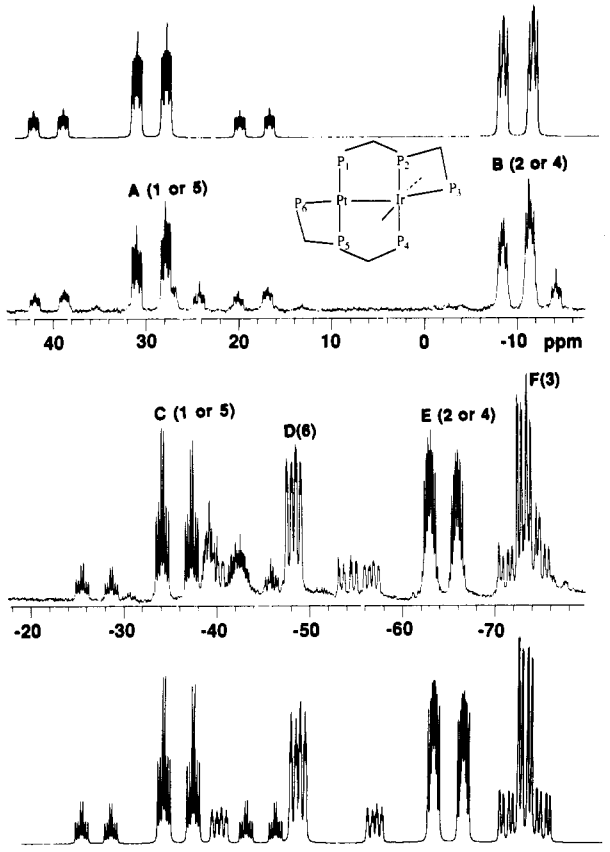

Figure 6. The 121.7-MHz $^{31}P\{^1H\}$ NMR spectrum of $[PtIr(CO)Cl(\mu\text{-dpmp})_2](PF_6)_2$ (**4**) in acetone-d_6 at 25 °C. The top and bottom are computed spectra with δ_A = 29.3 ppm, δ_B = −10.8 ppm, δ_C = −36.3 ppm, δ_D = −49.2 ppm, δ_E = −65.4 ppm, and δ_F = −73.6 ppm with J(A,B) = 40 Hz, J(A,C) = 383 Hz, J(A,D) = 18 Hz, J(A,E) = 65 Hz, J(A,Pt) = 2684 Hz, J(B,C) = 65 Hz, J(B,D) = 12 Hz, J(B,E) = 389 Hz, J(B,F) = 12 Hz, J(C,D) = 65 Hz, J(C,E) = −31 Hz, J(C,Pt) = 2142 Hz, J(D,F) = −121 Hz, J(D,Pt) = 2045 Hz, J(E,F) = 50 Hz, and J(F,Pt) = 485 Hz.

particularly in the −30 to −50 ppm region, so that a thorough analysis of the minor group is not warranted. It does appear, however, that they represent an isomeric form of **4** that is closely related in structure. One possibility for this isomer formation regards the relative locations of the CO and Cl ligands on iridium. Interchanging their locations from those seen in Figure 3 will produce a new but structurally similar isomer. Also the analysis given above makes no reference to conformation of the two dpmp ligands. The analysis holds regardless of whether the complex possesses the structure shown in Figure 3 or the structure in Figure 4 (with Pt replacing Pd). Thus, at this stage we cannot be sure that the relative dpmp conformations shown in Figure 3 represent the major or the minor species seen in solution.

The $^{31}P\{^1H\}$ NMR spectrum of $[PdIr(CO)Cl(\mu\text{-dpmp})_2](PF_6)_2$, **3**, resembles that of **4** in that six major resonances along with a set of minor resonances are seen. The overal pattern of major resonances is also preserved so that the structure in solution is consistent with the basic skeleton found in the solid state. The spectrum is reproduced in the supplementary material.

Electronic Absorption and Emission Spectra. The absorption data for $[Pd(dpmp)_2]^{2+}$ and $[Pt(dpmp)_2]^{2+}$ are similar with each showing a single absorption band in the ultraviolet region. The yellow dichloromethane solution of **1** has an absorbance at 328 nm (ϵ = 33 000 M^{-1} cm^{-1}) while the colorless solution of **2** has a shoulder at 326 nm (ϵ = 30 000 M^{-1} cm^{-1}). Neither **1** nor **2** are photoluminescent.

Relevant spectra for **3** and **4** are shown in Figures 7 and 8. The absorption spectrum of **3** in dichloromethane (trace A, Figure 7) shows a strong band at 458 nm (ϵ = 11 000 M^{-1} cm^{-1}) and a shoulder at 325 nm (ϵ = 10 000 M^{-1} cm^{-1}). The visible band is tentatively assigned to the $\sigma_{(M-M)} \rightarrow \sigma^*_{(M-M)}$ transition. Trace

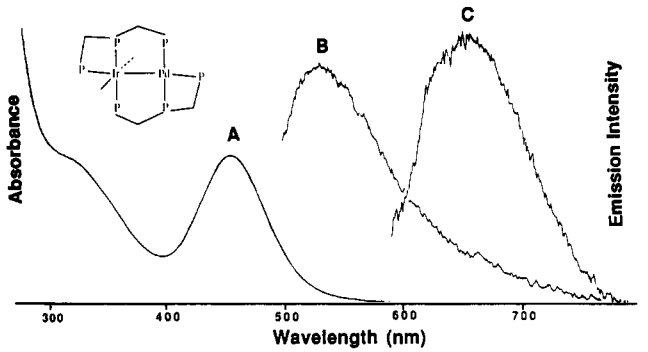

Figure 7. Electronic absorption (A) and uncorrected emission (B) spectra of $[PdIr(CO)Cl(\mu\text{-dpmp})_2](PF_6)_2$ (**3**) in dichloromethane at 25 °C. Trace C shows the emission spectrum obtained for a frozen solution at −196 °C.

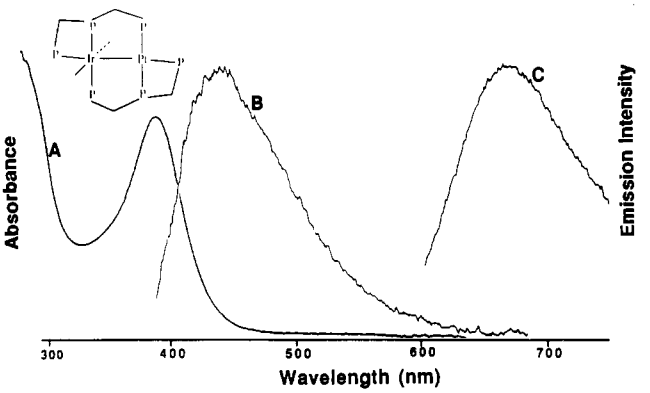

Figure 8. Electronic absorption (A) and uncorrected emission (B) spectra of $[PtIr(CO)Cl(\mu\text{-dpmp})_2](PF_6)_2$ in dichloromethane at 25 °C. Trace C shows the emission spectrum obtained for a frozen solution at −196 °C.

B represents the emission data gathered from a dichloromethane solution at 25 °C with excitation at 440 nm. There is a moderate emission at 520 nm. When the sample is frozen to −196 °C, the 520-nm emission disappears, and a new emission band appears at 665 nm (trace C). The emission lifetime of the 665-nm band at −196 °C is 5 μs, while the lifetime of the 520-nm band is shorter than our experimental observation (<350 ns). On the basis of the short lifetime and the small Stokes' shift, the 520-nm emission is assigned to a fluorescence process, while the lower energy 665-nm (−196 °C) emission with its long lifetime and large Stokes' shift is assigned to a phosphorescence process.

Comparison of the spectral data for **3** and **4** shows that the main absorption band of a 25 °C dichloromethane solution of **4** is at longer wavelength (382 nm (ϵ = 19 000 M^{-1} cm^{-1})) and sharper (trace A of Figure 8). Excitation into that band produces the moderate emission (trace B, Figure 8) at 443 nm. Freezing the sample to −196 °C causes the 443-nm band to disappear, and a new band at 670 nm appears (trace C). The lifetime of the 670-nm band in a frozen dichloromethane solution (−196 °C) is 27 μs. The feature is assigned to a phosphorescent process based on this long lifetime and its large shift to the red. The room temperature lifetime of the 443-nm emission is considerably shorter and escaped detection (<350 ns). This band is assigned to a fluorescent process.

Discussion

Both dpmp and the closely related bis((diphenylphosphino)-methyl)phenylarsine, dpma, are capable of forming strain-free, six-membered chelate rings as well as strained, four-membered chelate rings. $[Pd(dpmp)_2]^{2+}$ and $[Pt(dpmp)_2]^{2+}$ join a growing list of complexes that includes $[Ir(dpmp)_2(CO)]^{+}$[7] and $Ru(dpma)_2Cl_2$[17] which have the two ligands in different coordination modes; one acting to form a six-membered ring while the other

(17) Balch, A. L.; Olmstead, M. M.; Reedy, P. E., Jr.; Rowley, S. P. *Inorg. Chem.* **1988**, *27*, 4289.

forms a four-membered ring. Steric factors appear to be significant in creating this situation. The presence of two six-membered chelate rings produces a more crowded metal environment than one with one four-membered ring which pulls its two phosphine donors back from the metal by virtue of the narrow P–M–P angle of ca. 70°. In contrast, in $[Ir(dpma)_2(CO)]^{+}$[7] and in $[Au(dpma)_2]^{+}$,[15] both phosphine ligand adopt six-membered chelate ring forms.

Both $[Pd(dpmp)_2]^{2+}$ and $[Pt(dpmp)_2]^{2+}$ undergo chelate ring opening when treated with $Ir(CO)Cl(AsPh_3)_2$ to form the new 3:5 complexes, **3** and **4**. These products possess two four-membered chelate rings which themselves may be subject to chelate ring opening as demonstrated for complexes with chelating dpm ligands in the extensive studies of Shaw and co-workers.[18] Although these four-membered rings are stable under the conditions utilized, we are attempting to find conditions under which they may be opened to afford new polynuclear assemblages of higher nuclearity.

The structural properties of the two new 3:5 complexes are consistent with features previously identified for this structural class.[8] Thus, both have Ir–Pt or Ir–Pd distances that are fully consistent with the presence of a metal–metal single bond. As described previously, the metal–metal bonding in 3:5 complexes may be viewed in two ways.[8] If each metal retains the d^8 electronic configuration that it has in the precursor complexes, then the metal–metal bond is of the donor/acceptor type with the iridium acting as a two-electron donor to platinum or palladium. Alternatively, the metal–metal bond can be viewed as a covalent bond involving a d^9 platinum(I) or palladium(I) and a d^7 iridium(II). Since the carbon monoxide stretching vibrations for **3** (1996 cm^{-1}) and **4** (1977 cm^{-1}) show only a small increase relative to $Ir(CO)Cl(PPh_3)_2$ (1965 cm^{-1}), there is little evidence here for a substantial change in oxidation state for iridium, and the donor/acceptor view seems preferable.

Complexes **3** and **4** are the first complexes of the 3:5 structural type to show luminescence. The strong temperature dependence of the emission of each suggests that two excited states are involved. Phosphorescence is observed in frozen solutions at −196 °C, while solutions at 23 °C show fluorescence. The observed lifetimes are consistent with these assignments. While any assignment of the electronic absorption spectra must be offered cautiously since few data are available, it is tempting to suggest that the low energy absorption features at 458 nm in **3** and at 382 nm in **4** are the $\sigma \rightarrow \sigma^*$ transition within the metal–metal bond. These absorption bands are dependent on the metals involved, and the trend for the band to occur at lower energy for the second row metal (Pd) relative to the third row metal (Pt) is consistent with previous observations on $\sigma \rightarrow \sigma^*$ transitions.[18] The relatively low energies of these transitions in **3** and **4** may be related to the presence of phosphine ligands along the Ir–Pd or Ir–Pt axis and the strain involved in the off axial position of these terminal ligands.

Experimental Section

Preparation of Compounds. $PdCl_2(NCC_6H_5)_2$,[20] dpmp,[4] and dpma[7] were prepared by published methods. All new compounds reported here are stable to both moisture and air and were made without recourse to inert atmosphere techniques.

$[Pd(dpmp)_2](PF_6)_2$ (1). An orange solution of 189 mg (0.49 mmol) of $PdCl_2(NCPh)_2$ dissolved in 10 mL of dichloromethane was carefully added to 500 mg (0.99 mmol) of dpmp dissolved in 100 mL of hot ethanol. The solution quickly turned yellow. After 30 min of stirring, 200 mg (1.20 mmol) of ammonium hexafluorophosphate dissolved in 30 mL of methanol was added. The solution was stirred for 10 additional min and then was filtered through celite. The volume was reduced to yield a pale yellow crystalline solid which was collected by filtration, washed with diethyl ether, and vacuum dried. Yield: 85%.

$[Pt(dpmp)_2](PF_6)_2$ (2). This preparation is modeled after the preparation of **1** except 203 mg (0.49 mmol) of K_2PtCl_4 in a minimum volume of H_2O is used instead of $PdCl_2(NCPh)_2$. Addition of K_2PtCl_4 to a hot ethanol solution of dpmp resulted in a pale yellow solution. After the mixture was stirred for 20 min, 300 mg (1.84 mmol) of ammonium hexafluorophosphate dissolved in 30 mL methanol was added, and a white precipitate formed. The solid was collected by filtration, washed with methanol, and vacuum dried. Recrystallization was achieved by dissolution in a minimum volume of dichloromethane and precipitation with 2-propanol. Yield: 86%. Anal. Calcd for $PtC_{64}H_{58}P_8F_{12}$: C, 51.33; H, 3.90; P, 16.54; Cl, 0.0. Found C, 50.94; H, 3.97; P, 16.10; Cl, 0.0.

$[PdIr(CO)Cl(\mu\text{-dpmp})_2](PF_6)_2$ (3). To the solution formed by dissolving 150 mg (0.106 mmol) of $[Pd(dpmp)_2](PF_6)_2$ in 25 mL of acetone, 93 mg (0.100 mmol) of $Ir(CO)Cl(AsPh_3)_2$ was added. The solution turned orange and was stirred for 20 min. Then 100 mg (0.613 mmol) of ammonium hexafluorophosphate was added. The solution was stirred for 10 additional min. After the volume was reduced and ethyl ether was added, a red-orange, crystalline precipitate formed. The solid was collected by filtration, washed with ethyl ether, and dried in air. Recrystallization was achieved by dissolution in a minimum volume of dichloromethane and precipitation with ethyl ether. Yield: 81%. If $Ir(CO)Cl(PPh_3)_2$ were used instead of $Ir(CO)Cl(AsPh_3)_2$, the solution was boiled for 30 min before the ammonium hexafluorophosphate was added. The workup was identical to the arsine method.

$[PtIr(CO)Cl(\mu\text{-dpmp})_2](PF_6)_2$ (4). This preparation is identical to that of the palladium analog except that $[Pt(dpmp)_2](PF_6)_2$ was used, and the solution was boiled for 30 min. Yield: 80%.

Physical Measurements. The $^{31}P\{^1H\}$ NMR spectra were recorded on a General Electric QE-300 NMR spectrometer operating at 121.7 MHz with an external 85% phosphoric acid standard and the high field positive convention for reporting chemical shifts. Infrared spectra were recorded on an IBM IR-32 spectrometer. Electronic spectra were obtained with a Hewlett-Packard 8450A spectrometer. Uncorrected emission spectra were collected through the use of a Perkin-Elmer MPF-44B fluorescence spectrometer. Lifetime measurements were obtained as previously described.[7]

X-ray Crystallographic Studies. $[Pd(dpmp)_2](PF_6)_2 \cdot 0.5CH_2Cl_2$ (1). Yellow crystalline blocks were formed by slow diffusion of ethyl ether into a dichloromethane solution of $[Pd(dpmp)_2](PF_6)_2$. The air-sensitive crystals were coated with a light hydrocarbon oil to prevent cracking. The crystal was mounted on a glass fiber with silicone grease and placed in the 130 K nitrogen stream of a Siemens R3 diffractometer equipped with a modified Enraf-Nonius low temperature apparatus. Unit cell parameters were determined by least-squares refinement of 30 reflections with $8.7° < 2\theta < 26.8°$. The two check reflections exhibited only random fluctuations (<2%) during the data collection. The data were corrected for Lorentz and polarization effects. Crystal data are given in Table III.

Calculations were performed with SHELXTL version 4.11 installed on a Microvax computer. Scattering factors and corrections for anomalous dispersion were taken from a standard source.[22] The structure was solved by Patterson techniques. An absorption correction was applied.[23] The Pd, P, F, and Cl atoms were refined with anisotropic thermal parameters. The hydrogen atom positions were calculated by using a riding model with a C–H vector fixed at 0.96 Å and a thermal parameter 1.2 times the host carbon. The largest peak in the final difference map had density equal to 2.19 electrons/Å^3. This peak is 1.373 Å from P(6). One of the hexafluorophosphate anions was disordered and was modeled as two PF_6^- ions sharing the central phosphorus atom with 12 fluorine atoms at 50% occupancy.

$[Pd(dpmp)_2](PF_6)_2 \cdot (CH_3CH_2)_2O$ (1'). Apricot-colored blocks were formed by addition of ethyl ether to the ethanolic mother liquor from the original synthesis of **1**. These crystals were handled and mounted as described above. Unit cell parameters were determined by least-squares refinement of 12 reflections with $10.7° < 2\theta < 23.2°$. The two check reflections exhibited only random fluctuations (<2%) during the data collection. The data were corrected for Lorentz and polarization effects. Crystal data are given in Table III.

Calculations were performed as outlined above. The structure was solved by direct methods in the $C2/c$ (No. 15) space group. Hydrogen atoms were treated as described previously. The largest peak in the final difference map had density equal to 2.28 electrons/Å^3. This peak is located at (0.25, 0.75, 0) with no contacts within 4.0 Å.

$[PdIr(CO)Cl(\mu\text{-dpmp})_2](PF_6)_2 \cdot CHCl_3 \cdot CH_3OH$ (3). Red/gold dichroic parallelepipeds were grown by slow diffusion of diethyl ether through a 2-mm layer of methanol into a chloroform solution of $[PdIr(CO)Cl(\mu\text{-dpmp})_2](PF_6)_2$. The crystals were handled and a suitable specimen

(18) Blagg, A.; Cooper, G. R.; Pringle, P. G.; Robson, R.; Shaw, B. L. *J. Chem. Soc., Chem. Commun.* **1984**, 933.
(19) Levenson, R. A.; Gray, H. B. *J. Am. Chem. Soc.* **1975**, *97*, 6042.
(20) Holden, J. R.; Baenziger, N. C. *Acta Crystallogr.* **1956**, *9*, 194.
(21) Balch, A. L.; Fossett, L. A.; Olmstead, M. M.; Oram, D. E.; Reedy, P. E., Jr. *J. Am. Chem. Soc.* **1985**, *107*, 5272.
(22) *International Tables for X-ray Crystallography*; Kynoch Press: Birmingham, England, 1974; Vol. 4.
(23) The method obtains an empirical absorption tensor from an expression relating F_o and F_c: Moezzi, B. Ph.D. Thesis, University of California, Davis, 1987.

mounted as described above. Unit cell parameters were determined by least-squares refinement of 13 reflections with $6.1° < 2\theta < 18.4°$. The two check reflections show only random fluctuations (<2%) throughout the data collection. The data were corrected for Lorentz and polarization effects. Crystal data are given in Table III.

Based on the observed condition $0k0$, $k = 2n$, two space groups, $P2_1$ (No. 4) and $P2_1/m$ (No. 11) were possible. The chiral space group $P2_1$ (No. 4), was chosen based on the absence of a crystallographic mirror plane. The structure was solved using direct methods and refinement followed procedures outlined above. The absolute configuration was determined by adding the parameter, η, to the atomic scattering factors.[24] Subsequent refinement led to an η of 1.01 (6). An absorption correction was applied.[22] Final refinement was carried out with anisotropic thermal parameters for all non-hydrogen atoms of the cation except O(1) and the carbon atoms. Hydrogens were fixed to the methylene carbons of the two dpmp ligands and to the $CHCl_3$ in a fashion previously outlined. The largest peak in the final difference map had density equal to 1.13 electrons/Å^3. This peak is 0.924 Å from F(8).

$[PtIr(CO)Cl(\mu\text{-dpmp})_2](PF_6)_2\cdot 0.75CH_2Cl_2$ (4). Yellow pyramids were obtained by slow diffusion of diethyl ether into a dichloromethane solution of $[PtIr(CO)ClPd(\mu\text{-dpmp})_2](PF_6)_2$. The crystals were handled and mounted as previously described. Unit cell parameters were determined by least-squares refinement of 23 reflections with $7.5° < 2\theta < 22.4°$. The monoclinic crystal system and the cell parameters were verified by examination of axial photo data. The two check reflections showed only random fluctuations (<2%) during the data collection. The data were corrected for Lorentz and polarization effects. Crystal data are given in Table III.

The structure was solved in the centrosymmetric space group, $P2_1/n$ (No. 14). Platinum and iridium atomic positions were determined from a Patterson map. Refinement and calculations were performed as described above. There exists a heavily disordered dichloromethane molecule in the structure at 75% occupancy. This was best modeled with one carbon atom, C(66), sharing a position with a chlorine at 25% occupancy and five other chlorines each at 25% occupancy. The largest peak in the final difference map is equivalent to 3.60 electrons/Å^3. This peak is 1.119 Å from Pt(1).

Acknowledgment. We thank the National Science Foundation (CHE-894209 and CHE-9022909) for support and Johnson Matthey, Inc., for a loan of platinum and iridium salts. V.J.C. thanks the International Precious Metals Institute for a fellowship and Dr. Marilyn M. Olmstead and Bruce C. Noll for assistance with crystallography.

Supplementary Material Available: $^{31}P\{^1H\}$ NMR spectrum of **3** and tables of atomic coordinates, bond distances, bond angles, anisotropic thermal parameters, hydrogen atom positions, and crystal data for **1**, **1'**, **3**, and **4** (55 pages); listings of observed and calculated structure factors (103 pages). Ordering information is given on any current masthead page.

(24) Rogers, D. *Acta Crystallogr.* **1981**, *A37*, 734.

Contribution from the Department of Chemistry, University of Southampton, Southampton SO9 5NH, U.K., and Department of Pure and Applied Chemistry, University of Strathclyde, Glasgow G1 1XL, U.K.

Coordination Chemistry of Higher Oxidation States. 39.[1] Structural and Spectroscopic Studies on Manganese(IV) Periodato Complexes. Crystal Structure of $Na_7[Mn(HIO_6)_2(H_2IO_6)]\cdot 18H_2O$

William Levason,*[,2a] Mark D. Spicer,[2b] and Michael Webster[2a]

Received September 5, 1991

The reaction of MIO_4 (M = Na, K, Rb, or Cs) with a manganese(II) salt in acidic aqueous solution at 40 °C produces insoluble dark red-brown manganese(IV) complexes $MMnIO_6\cdot nH_2O$. In contrast NaOCl oxidation of a manganese(II) salt in alkaline solution in the presence of $NaIO_4$ affords soluble red crystals of $Na_7[Mn(H_2IO_6)(HIO_6)_2]\cdot 18H_2O$. This crystallizes in the orthorhombic system, space group *Pnca* (a = 10.281 (7) Å, b = 15.971 (2) Å, c = 19.564 (2) Å, Z = 4, V = 3212 Å^3). The structure of the anion reveals octahedrally coordinated Mn, chelated by two $O_2IO_3(OH)^{4-}$ and one *trans*-$O_2IO_2(OH)_2^{3-}$ groups, and is the first structurally characterized example of a coordinated $H_2IO_6^{3-}$ group. EXAFS (Mn K- and I L_{III} edge) studies on the $MMnIO_6\cdot nH_2O$ gave Mn-O = 1.89 Å, I-O = 1.92 Å, and Mn···I = 2.89 Å. UV-visible spectroscopy and magnetic data are reported and confirm all the complexes contain Mn(IV). Attempts to obtain periodate complexes of Mn(III) or of oxidation states Mn(≥5) have been unsuccesful. Spectroscopic and EXAFS data are also reported for the hexakis(iodate) complex $K_2[Mn(IO_3)_6]$.

Introduction

Periodate $(H_{5-n}IO_6)^{n-}$ and tellurate $(H_{6-n}TeO_6)^{n-}$ anions are highly effective ligands for stabilizing high oxidation states of the transition metals, often as water-soluble anions, which in addition to their inherent interest have found uses as multielectron oxidants and in chemical analysis.[3-7] A number of manganese periodate complexes have been reported previously,[8] and we report here some new examples and a detailed structural (X-ray and EXAFS) and spectroscopic reinvestigation of known complexes. The high oxidation state chemistry of manganese has been reviewed several times,[9] and particular recent interest attaches to complexes with N and/or O donor ligands which may function as models for the manganese site in photosystem II.[9c]

Experimental Section

Spectroscopic measurements were made as described previously.[1,4,5] IR spectra were obtained from Nujol mulls, and samples for diffuse reflectance spectra were diluted with barium sulfate. Samples were dried in vacuo (10^{-3} Torr) at room temperature for 24 h. The approximate composition of the complexes was established by energy dispersive X-ray fluorescence spectroscopy. For conventional analyses, known weights of the complexes were dissolved/suspended in hot 2 mol dm^{-3} sulfuric acid, and sulfur dioxide was bubbled in until a colorless solution was formed.

(1) Part 38. Champness, N. R.; Levason, W.; Mould, R. A. S.; Pletcher, D.; Webster, M. *J. Chem. Soc., Dalton Trans.* **1991**, 2777.
(2) (a) University of Southampton. (b) University of Strathclyde.
(3) El-Hendawy, A. M.; Griffith, W. P.; Piggott, B.; Williams, D. J. *J. Chem. Soc., Dalton Trans.* **1988**, 1983.
(4) Levason, W.; Spicer, M. D.; Webster, M. *Inorg. Chem.* **1991**, *30*, 967.
(5) Levason, W.; Spicer, M. D.; Webster, M. *J. Coord. Chem.* **1991**, *23*, 67.
(6) Adelskold, V.; Eriksson, L.; Wang, P.-L.; Werner, P.-E. *Acta Crystallogr. Sect. C* **1988**, *C44*, 597.
(7) Balikungeri, A.; Pelletier, M.; Monier, D. *Inorg. Chim. Acta* **1977**, *22*, 7; **1978**, *29*, 137.
(8) *Gmelin Handbuch der Anorganische Chemie, Teil 56 Mangan*; Springer: Berlin, 1978; Vol. C5, p 339.
(9) (a) Levason, W.; McAuliffe, C. A. *Coord. Chem. Rev.* **1972**, *7*, 353. (b) Chiswell, B. C.; McKenzie, E. D.; Lindoy, L. F. In *Comprehensive Coordination Chemistry*; Wilkinson, G., Gillard, R. D., McCleverty, J. A., Eds.; Pergamon: New York, 1987; Vol. 4, p 1. (c) Brudwig, G. W.; Crabtree, R. H. *Prog. Inorg. Chem.* **1989**, *37*, 99.

0020-1669/92/1331-2575$03.00/0